The Astrophysical Journal, 634:1372–1384, 2005 December 1

A *SPITZER* STUDY OF DUSTY DISKS AROUND NEARBY, YOUNG STARS

C. H. Chen,[1,2,3] B. M. Patten,[4] M. W. Werner,[1] C. D. Dowell,[1] K. R. Stapelfeldt,[1] I. Song,[5] J. R. Stauffer,[6] M. Blaylock,[7] K. D. Gordon,[7] and V. Krause[8]

Received 2005 May 18; accepted 2005 August 3

ABSTRACT

We have obtained *Spitzer Space Telescope* MIPS (Multiband Imaging Photometer for *Spitzer*) observations of 39 A- through M-type dwarfs, with estimated ages between 12 and 600 Myr; IRAC observations for a subset of 11 stars; and follow-up CSO SHARC II 350 μm observations for a subset of two stars. None of the objects observed with IRAC possess infrared excesses at 3.6–8.0 μm; however, seven objects observed with MIPS possess 24 and/or 70 μm excesses. Four objects (κ Phe, HD 92945, HD 119124, and AU Mic), with estimated ages 12–200 Myr, possess strong 70 μm excesses, $\geq$100% larger than their predicted photospheres, and no 24 μm excesses, suggesting that the dust grains in these systems are cold. One object (HD 112429) possesses moderate 24 and 70 μm excesses with a color temperature, $T_{\rm gr} = 100$ K. Two objects (α^1 Lib and HD 177724) possess such strong 24 μm excesses that their 12, 24, and 70 μm fluxes cannot be self-consistently modeled using a modified blackbody despite a 70 μm excess >2 times greater than the photosphere around α^1 Lib. The strong 24 μm excesses may be the result of emission in spectral features, as observed toward the Hale-Bopp star HD 69830.

Subject headings: circumstellar matter — planetary systems: formation

Online material: color figure

1. INTRODUCTION

The observation of periodic variations in the radial velocities of nearby late-type stars has led to the discovery of ~140 giant planets (Marcy et al. 2000), including 14 multiple planet systems, suggesting that planetary systems may be common. Giant planets, such as Jupiter, are believed to form in protoplanetary disks made of gas and dust. Circumstellar disks have been resolved in a handful of nearby, young stellar associations: the TW Hydrae association, which contains TW Hya and HR 4796A; the β Pic moving group, which contains β Pic and AU Mic; and the Castor moving group, which contains Fomalhaut, Vega, and ζ Lep. High-resolution imaging studies of disks around these members have discovered structures that suggest that planets may be forming or may have already formed in these systems. For example, scattered light and thermal infrared imaging has discovered a central clearing in the HR 4796A disk (Schneider et al. 1999; Jayawardhana et al. 1998), and warps and rings in the β Pic disk (Telesco et al. 2005; Wahhaj et al. 2003; Heap et al. 2000), while far-infrared and submillimeter imaging has discovered a central clearing in the cold dust around Fomalhaut (Marsh et al. 2005; Stapelfeldt et al. 2004; Holland et al. 2003).

Stellar members of moving groups, such as the TW Hydrae association, the β Pic moving group, and the Castor moving group, are identified via signatures of youth (i.e., high X-ray flux, large lithium abundance, and strong chromospheric activity) and common proper motions (Zuckerman & Song 2004; Zuckerman et al. 2001; Barrado y Navascués 1998), suggesting that they formed recently in the same region. The ages of these groups are fairly well determined, primarily on the basis of the properties of their low-mass members in comparison to members of well-studied open clusters. The moving groups are generally closer to the Sun than the calibrating open clusters, and hence they provide excellent laboratories for study of the evolution of dusty debris disks around young, main-sequence stars as a function of age and stellar mass. We have carried out a *Spitzer Space Telescope* search for infrared excesses, believed to be generated by thermal emission from circumstellar dust, around members of stellar moving groups. Follow-up coronagraphic imaging of infrared excess sources, including HD 92945 in this sample, has revealed the presence of extended circumstellar disks.

One goal toward understanding how planets form around young stars is understanding the dust dissipation timescales in these systems. The excellent sensitivity of the *Spitzer* satellite will enable a comprehensive study of the disappearance of dust around solar-type main-sequence stars. Already *Spitzer* MIPS observations of main-sequence A-type stars suggest that 24 μm excess declines with a time dependence, ~150 Myr/t (Rieke et al. 2005), consistent with collisionally replenished disks (Dominik & Decin 2003), but that as many as 50% of young A-type stars do not possess excess emission. The first results from *Spitzer* MIPS surveys of nearby, solar-type, main-sequence stars suggest that the disk fraction in the ~10 Myr old TW Hydrae association is 25% (Low et al. 2005), while the disk fraction in the 3–20 Myr old Scorpius-Centaurus OB association may be as high as 50% (Chen et al. 2005). The 100 Myr old open cluster M47 (NGC 2422) has a disk fraction ~15% (Gorlova et al. 2004), commensurate with the frequency of debris disks around main-sequence stars (Lagrange et al. 2000). A volume-limited survey of solar-type field stars within 25 pc suggests that debris disks can persist to ages $\geq$6 Gyr (Beichman et al. 2005a).

In this paper we report on the initial results from a *Spitzer* guaranteed time program to search for debris disks around 69 nearby, young stars. We have obtained MIPS 24 and 70 μm

[1] Jet Propulsion Laboratory, California Institute of Technology, 4800 Oak Grove Drive, Pasadena, CA 91109.
[2] Department of Physics and Astronomy, University of California, Los Angeles, CA 90095-1562.
[3] NOAO, 950 North Cherry Avenue, Tucson, AZ 85719; cchen@noao.edu.
[4] Harvard-Smithsonian Center for Astrophysics, 60 Garden Street, Cambridge, MA 02138-1516.
[5] Gemini Observatory, 670 North A'ohoku Place, Hilo, HI 96720.
[6] *Spitzer* Science Center, California Institute of Technology, Mail Code 314-6, Pasadena, CA 91125.
[7] Steward Observatory, University of Arizona, Tucson, AZ 85721.
[8] Division of Physics, Math, and Astronomy, California Institute of Technology, MS 103-33, Pasadena, CA 91125.

TABLE 1
STELLAR PROPERTIES

Name	HD/HDE	Spectral Type	Distance (pc)	*ROSAT* (counts s^{-1})	$\dot{M}_{wind}$ ($\dot{M}_\odot$)[a]	t_{age} (Myr)	Association[b]	References
BE Cet	1835	G3 V	20	0.289	95	600	HSC	1
κ Phe	2262	A7 V	24	...	...	200	CMG	2
BB Scl	9770[c]	K3 V	24	2.59	1600			
	10008	G5	24	0.440	70	20–150	LA	1
	29697	K3 V	14	2.36	520	500	UMG	3
	11131[d]	G0	23	0.386	160			
Gl 182		M0	27	0.651	480	20–150	LA	4
AB Dor	36705	K1 III	15	7.22	2400	50–100	ABDMG	5, 6
RST 137B		M3.5 Ve	15	...	...	50–100	ABDMG	6, 7
Gl 226.2		K8 V	25	0.064	26	200	CMG	1, 2
Gl 3400A	48189	G1.5 V	22	2.33	1300	50–100	ABDMG	5, 6
Gl 255AB[d]		F8 IV–V	...	0.412	910	200	CMG	1, 2
	51849	K4 V	22	0.503	270			
Castor	60178[d]	A2 Vm	16	3.70	...	200	CMG	2
	74576	K1 V	11	0.460	41			
Gl 351A	82434[d]	F3 IV	...	0.558	130	200	CMG	1, 2
	92139	F4 IV+	27	0.203	84	50		8, 9
	92945	K1 V	22	0.118	47	20–150	LA	1
	105963	K0	27	0.150	80			
	112429	A5n[e]	29	0.0261	...	50		8, 9
	119124[d]	F8 V	25	0.365	220	200	CMG	1, 2
α^1 Lib	130819[d]	F3 V	23	0.283	120	200	CMG	1, 2
	141272	G8 V	21	0.0375	12	20–150	LA	1
RE 1816+541		dM1-2e	...	0.292	80	20–150	LA	10
	175742	K0	21	1.88	1200	500	UMG	3
ζ Aql	177724[d]	A0 V	26	0.141	...	83		8, 9
	180161	G8 V	20	0.155	56			
	186219	A4 III	42	0.0897	...	50		8, 9
AT Mic	196982[d]	M4.5	10	3.91	450	12	BPMG	4
η Ind	197157	A6:var	24	...	...	50		8, 9
AU Mic	197481	M0	10	5.95	720	12	BPMG	4
BO Mic	197890	K0 V	44	6.11	25000	20–150	LA	1
	358623	K7 V:e	...	0.236	820	<20	BPMG	11
Alderamin	203280	A7 IV	15	0.019	...	200	CMG	2
CPD-53 10037AB	202730[d]	A5 V	30	0.419	...	50		8, 9
LO Peg		K8	25	0.923	620	50–100	ABDMG	5, 6
	212697	G3 V	20	0.847	320			
HK Aqr		M0	22	0.427	200	200	CMG	1, 2
KZ And	218738	G5	25	1.93	1600			
Gl 907.1		K8	27	0.404	280	35–55	IC 2391MG	1

[a] $\dot{M}_\odot = 3 \times 10^{-14}\ M_\odot\ \mathrm{yr}^{-1}$.
[b] BPMG = β Pic moving group; IC 2391MG = IC 2391 moving group; ABDMG = AB Dor moving group; LA = Local Association; CMG = Castor moving group; UMG = Ursa major group; and HSC = Hyades supercluster.
[c] Triple.
[d] Binary.
[e] Spectral type: A5n (Royer et al. 2002). Other spectral types for this star: F0 IV–V (Gray & Garrison 1989); F1 (Fekel et al. 2003); F1VmA7(n) (Gray et al. 2003).

REFERENCES.—(1) Montes et al. 2001; (2) Barrado y Navascués 1998; (3) King et al. 2003; (4) Liu et al. 2004; (5) Zuckerman et al. 2004; (6) Luhman et al. 2005; (7) Lim 1993; (8) Song et al. 2001; (9) Song 2000; (10) Jeffries et al. 1994; (11) Kaisler et al. 2004.

photometry for 39 (spectral types A–K) stars so far and Infrared Array Camera (IRAC) 3.6, 4.5, 5.8, and 8.0 μm photometry for a subset of these objects (11 objects with spectral types G–M). The stars observed include three members of the 12 Myr old β Pic moving group (Zuckerman et al. 2001), five members of the 20–100 Myr old Local Association (Montes et al. 2001), three members of the 50–100 Myr old AB Doradus moving group (Luhman et al. 2005; Zuckerman et al. 2004), and nine members of the 200 Myr Castor moving group (Montes et al. 2001; Barrado y Navacués 1998). The membership of these stars in their respective associations has been determined using a suite of youth indicators, including high lithium abundance, high coronal X-ray activity, and common proper motion. We list the targets along with their spectral types, distances, *ROSAT* (*Röntgensatellit*) fluxes, and moving group memberships in Table 1.

2. OBSERVATIONS

2.1. *IRAC Observations*

Our "short-wavelength" observations were obtained using the IRAC (Fazio et al. 2004) on *Spitzer* (Werner et al. 2004). The IRAC data were obtained primarily in support of a separate GTO program designed to search for low-mass and substellar mass companions to nearby young stars (PID 34; PI: G. G. Fazio). To support the deep imaging needed for the companion

TABLE 2
IRAC 3.6, 4.5, 5.8, AND 8.0 μm FLUXES

Name	AOR ID	F_ν(3.6 μm) (mJy)	F_ν(4.5 μm) (mJy)	F_ν(5.8 μm) (mJy)	F_ν(8.0 μm) (mJy)
HD 10008	3930112	...	...	554 ± 7	316 ± 1
HD 29697	3917312	...	...	1070 ± 11	619 ± 7
HD 11131	3930624	...	...	992 ± 9	565 ± 3
Gl 182	3917568	...	610 ± 12	411 ± 6	234 ± 1
AB Dor	3918080	...	...	1600 ± 13	896 ± 7
RST 137B	3918080	465 ± 8	310 ± 6	209 ± 2	118 ± 2
HD 48189	3918592	...	...	1894 ± 24	1079 ± 14
HD 92945	3920640	...	...	630 ± 6	360 ± 2
RE 1819+541	3923200	248 ± 5	160 ± 2	108 ± 2	60 ± 1
AU Mic	3925248	...	...	2236 ± 56	1312 ± 21
BO Mic	3925504	...	368 ± 7	242 ± 3	142 ± 1
LO Peg	3926016	...	515 ± 13	344 ± 6	197 ± 2

NOTE.—The uncertainties listed here are formal statistical uncertainties and do not include the ~2% uncertainty in IRAC calibration.

search program while also providing useful photometry for the relatively bright target stars in at least the 8.0 μm channel in support of the debris disk study, IRAC's high dynamic range mode was used with 2 and 30 s FRAMETIME images made at each dither position. The basic observation for all targets in the program were identical. Each target position was observed through both IRAC fields of view using a five-position Gaussian dither pattern with a maximum offset in the pattern from the center/initial position of ~38″.

Starting with the basic calibrated data (BCD) produced by the IRAC pipeline software at the *Spitzer* Science Center, the individual dithered images were co-added to increase the overall signal-to-noise ratio (S/N) of the target with clipping to remove transients such as cosmic rays. Net source counts for the target stars were extracted from the co-added BCD data at the target position using routines in the IRAF `apphot` package. For most of the targets, a source aperture of 10 pixel radius was used, with sky background removed using an annulus with inner radius of 10 pixels and a width of 10 pixels. For three of the stars, crowding forced us to use a 4 pixel radius source aperture. In these cases an aperture correction factor had to be applied to the net flux for each channel (1.080, 1.085, 1.069, and 1.073, respectively). Error estimates were made based on the repeatability of the photometry (the standard deviation) of the target stars in the individual BCD frames in the dither pattern. The calibration of the IRAC photometry is based on the calibration applied to the BCD data by the *Spitzer* Science Center for the S10 version of the IRAC pipeline (given in units of MJy sr^{-1}) combined with the known solid angles of the IRAC pixels in each of the 4 IRAC channels.

We list the observed 3.6, 4.5, 5.8, and 8.0 μm fluxes in Table 2. We plot the Two Micron All Sky Survey (2MASS) $J - H$ versus $H - K$ and the IRAC/2MASS $J - H$ versus [5.8] − [8.0] color-color diagrams in Figures 1*a* and 1*b*, respectively. The colors of

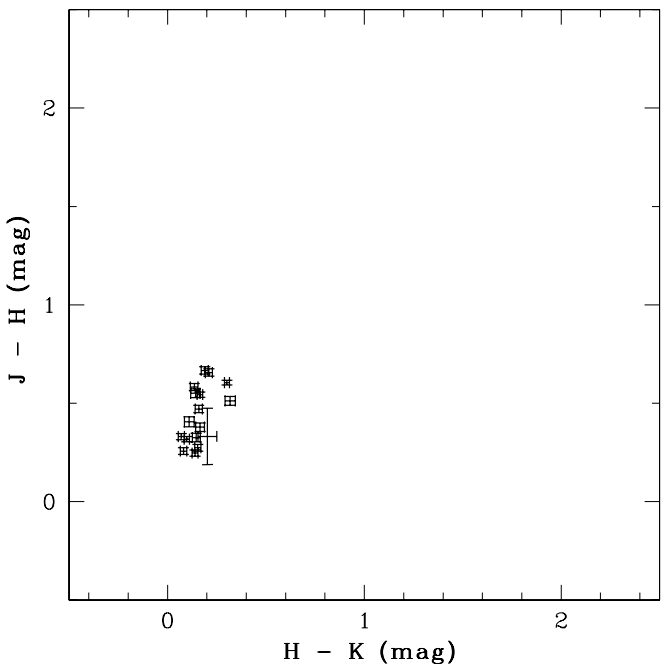

FIG. 1*a*

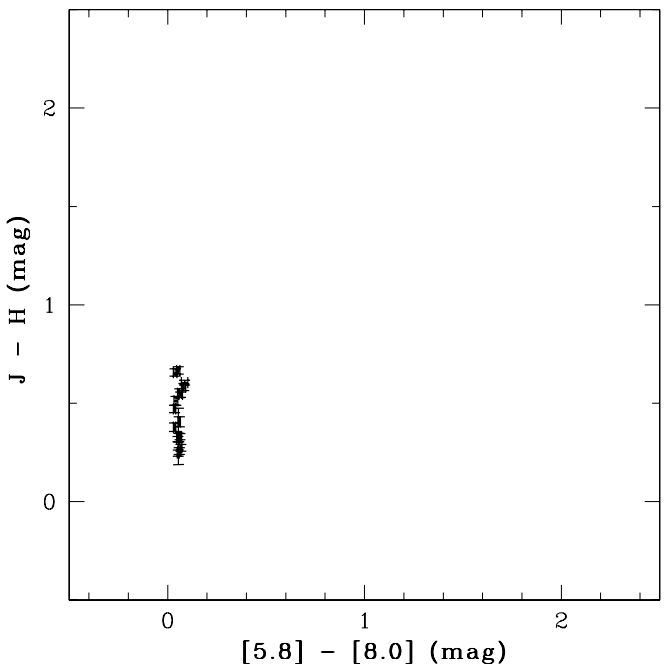

FIG. 1*b*

FIG. 1.—(*a*) 2MASS $J - H$ vs. $H - K$ color-color diagram and (*b*) 2MASS/IRAC $J - H$ vs. [5.8] − [8.0] color-color diagram. The colors of all sources are consistent with main-sequence stars.

TABLE 3
MIPS 24 μm AND 70 μm FLUXES (NOT COLOR-CORRECTED)

Name	AOR ID	Measured MIPS F_ν(24 μm) (mJy)	Predicted Photosphere F_ν(24 μm) (mJy)	χ_{24}	Measured MIPS F_ν(70 μm) (mJy)	Measured 70 μm S/N	Predicted Photosphere F_ν(70 μm) (mJy)	χ_{70}	*COBE* 70 μm Background (MJy sr^{-1})
Stars with MIPS Excesses									
κ Phe	6036736	297	337	−1.4	64.1	28	32.2	2.5	6.8
HD 92945	4640256	39.2	42.7	−0.9	271	84	4.5	4.9	9.1
HD 112429	4627712	125	107	1.4	52.2	12	11.9	3.9	5.7
HD 119124	6038528	70.6	82.4	−1.7	56.1	21	7.9	4.3	5.8
α^1 Lib	6037760	752	190	7.5	69.3	27	18.3	3.7	21.1
HD 177724	4631296	475	299	3.7	32.9	4	32.3	0.1	25.7
AU Mic	4637440	151	153	−0.1	196	43	22.5	4.4	15.1
Stars without MIPS Excesses									
BE Cet	4631808	82.7	90.5	−0.9	19.3	6	10.2	2.4	15.4
BB Scl	4640768	84.6	109	−2.9	<12.3	...	12.4	...	7.9
HD 10008	4626944	38.7	41.1	−0.6	22.1	5	4.7	3.9	13.9
HD 29697	4638464	67.5	82.8	−2.3	<27.5	...	9.3	...	25.6
HD 11131	4627456	63.6	68.2	−0.7	<12.6	...	7.7	...	12.1
Gl 182	4635392	27.4	31.2	−1.4	<14.1	...	4.6	...	13.1
AB Dor/RST 137B	4638720	114	106	0.7	<16.0	...	12.2	...	7.0
Gl 226.2	6036992	16.6	19.8	−1.9	<7.5	...	2.8	...	9.0
HD 48189	4639232	112	115	−0.3	<16.6	...	13.1	...	5.9
Gl 255AB	6038272	63.8	76.9	−2.1	<15.5	...	7.4	...	10.8
HD 51849	4639488	26.5	31.5	−1.9	<13.5	...	3.6	...	13.6
Castor	6037248	...	2170	...	154	39	207	−1.7	17.1
HD 74576	4640000	125	146	−1.7	19.2	7	16.7	0.7	16.9
Gl 351AB	6038016	608	775	−2.8	65.2	19	74.5	−0.7	11.7
HD 92139	4634880	399	425	−0.7	49.0	13	47.0	0.2	11.1
HD 105963	4636160	40.4	38.5	0.5	<9.6	...	4.4	...	6.7
HD 141272	4629760	42.1	51.0	−2.1	<12.6	...	5.8	...	12.8
RE 1816+541	4641280	7.1	8.5	−2.0	<12.6	...	0.9	...	5.8
HD 175742	4636928	44.5	42.2	0.5	<9.7	...	4.8	...	12.4
HD 180161	4631552	56.4	72.3	−2.8	<12.1	...	8.2	...	6.7
HD 186219	4626688	85.8	86.2	−0.1	18.0	8	9.4	2.4	7.1
AT Mic	4637184	124	124	0.0	21.8	5	13.3	2.0	14.4
η Ind	4632064	194	170	1.2	25.5	6	18.5	1.4	8.3
BO Mic	4637696	15.3	13.1	1.4	<12.0	...	1.5	...	12.3
HD 358623	4643840	13.4	10.5	2.2	<8.5	...	1.2	...	19.1
Alderamin	6037504	1260	1280	−0.2	112	33	120	−0.4	14.7
HD 202730[a]	4632320	197	288	−4.6	23.2	9	34.4	−2.4	7.6
LO Peg	4641024	22.3	20.8	0.7	<7.6	...	2.3	...	9.3
HD 212697	4637952	165	197	−1.9	25.8	6	22.3	0.7	17.6
HK Aqr	4635648	11.7	14.2	−2.1	<12.9	...	2.1	...	17.3
HD 218738	4638208	49.5	51.5	−0.4	<10.8	...	5.8	...	9.5
Gl 907.1	4635904	25.9	27.5	−0.6	<9.2	...	3.9	...	16.4

[a] Photosphere estimates are made assuming that both components of the binary system are at the same distance.

all of the objects observed using IRAC are consistent with main-sequence stars (Allen et al. 2004).

2.2. *MIPS Observations*

Our "medium" wavelength observations were obtained using the Multiband Imaging Photometer for *Spitzer* (MIPS; Rieke et al. 2004) on the *Spitzer Space Telescope* (Werner et al. 2004) in photometry mode at 24 and 70 μm (default scale). Each of our targets was observed in 2004, using integration times of 48.2 s at 24 μm and 186–465 s at 70 μm. The data were reduced and combined using the Data Analysis Tool (DAT; ver. 2.80) developed by the MIPS instrument team (Gordon et al. 2005). Extra processing steps beyond those in the DAT were applied to remove known transient effects associated with the 70 μm detectors to achieve the best possible sensitivity. While point sources are well calibrated using the stim flashes, extended sources (e.g., the background) show small responsivity drifts with respect to the point-source calibration. As a result, the background in uncorrected mosaics displays significant structure associated with detector columns. This detector-dependent structure is removed by subtracting column averages from each exposure with the source region masked. In addition, a pixel-dependent time filter is applied (with the source region masked) to remove small pixel-dependent residuals. These corrected images are then combined to produce the final mosaic used for the source detection.

The estimated 70 μm sky backgrounds, extrapolated from *COBE* (*Cosmic Background Explorer*) data, using the IRSKY

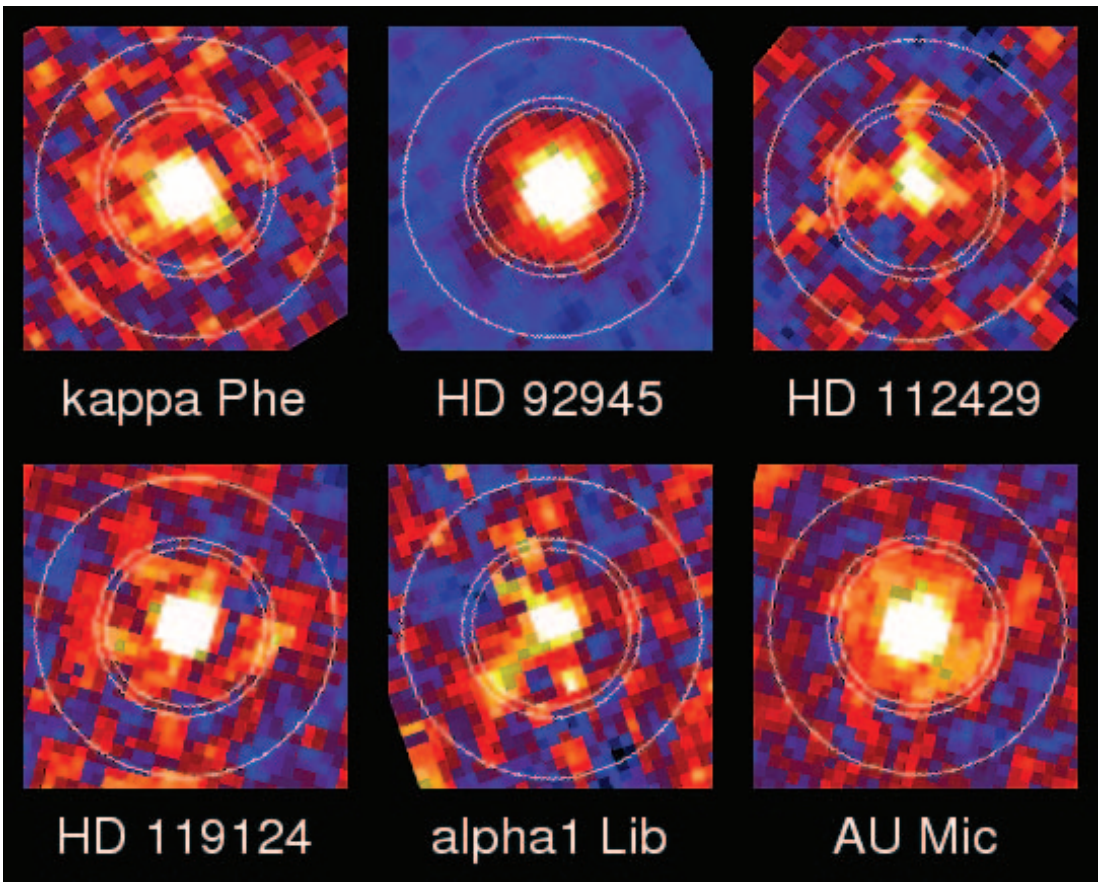

FIG. 2.—MIPS 70 μm images of sources with 70 μm excess. All of the images are rotated so that north is up and east is to the left. The inner circle has a radius of 30″ and shows the photometry aperture used. The outer annulus has an inner radius of 40″ and an outer radius of 80″, and shows the region used to estimate the sky background.

Batch Inquiry System (IBIS), suggest that our fields of view possess low to fairly high 70 μm cirrus backgrounds (see Table 3). If no object was detected at the center of the array, we placed 3 σ upper limits on the fluxes, where σ is the standard deviation of the sky in the background annulus. This sky noise includes detector noise and noise due to cirrus structures present in the image. If the observations were taken in regions with high cirrus, then the detection limits are dominated by cirrus noise. Examination of these 70 μm images reveals significant cirrus structures that make our simple aperture photometry detection limits conservative upper limits. All sources detected at 24 and at 70 μm (with S/N $>$ 10) appear as point sources with FWHM $\sim$ 5.″7 and $\sim$20″ at 24 and 70 μm, respectively. They also have positions coincident with *Hipparcos* stellar positions, suggesting that the far-infrared emission is circumstellar and not interstellar. Sources with 70 μm fluxes that are detected with S/N $<$ 10 do not have high enough S/Ns to determine whether the source is a point source or a bright peak in the cirrus background. The 70 μm images and radial profiles for sources with 70 μm excess are shown in Figures 2 and 3 so that the observed 70 μm sky can be seen.

We used aperture photometry to measure the fluxes, by finding the average brightness of a pixel in a "sky" annulus around the source, subtracting this value from each pixel in the aperture, and then summing the flux in the aperture. Since our observations are diffraction limited and the pixel scale for the 24 and 70 μm detectors are different, we use different aperture radii and sky annuli for the 24 and 70 μm data. At 24 μm, we used a 15″ (6 pixel) radius aperture and a sky annulus between 30″ and 43″ (12–17 pixels) radius. At 70 μm, the source aperture radius was 29.″5 (3 pixels) and the sky annulus was 40″–80″ (4–8 pixels). These apertures are not large enough to contain all of the photons from a diffraction-limited point source; therefore, we applied scalar aperture corrections of 1.147 and 1.741 at 24 and 70 μm, respectively, inferred from *Spitzer* Tiny Tim models of the point-spread function (Krist 2002), to extrapolate the object fluxes from the photon fluxes in the apertures. We flux calibrated our data assuming conversion factors of 1.042 μJy arcsec^{-2}/(DN s^{-1}) at 24 μm and 1.58×10^4 μJy arcsec^{-2}/(DN s^{-1}) at 70 μm. We list the observed 24 and 70 μm (not color-corrected) fluxes in Table 3. The results assume a λ^{-2} flux density across the MIPS bandpasses. Current observations of standard stars suggest that MIPS 24 μm photometry has an absolute calibration uncertainty of $\sim$10% for stars fainter than 4 Jy and that MIPS 70 μm photometry has an absolute calibration uncertainty of $\sim$20% for objects brighter than 50 mJy.

We estimated the stellar photospheric fluxes of our objects by minimum χ^2 fitting published photometry from the literature to model stellar atmospheres, using only bandpasses with wavelengths shorter than 3 μm. For stars with spectral types earlier than K2 V, we used 1993 Kurucz stellar atmospheres; for stars later than K2 V, we used Nextgen models. Where possible, we included fluxes from TD 1 (Thompson et al. 1978), *Hipparcos*, the General Catalogue of Photometric Data (GCPD; Mermilliod et al. 1997), and 2MASS (Cutri et al. 2003). For comparison with our measured (but not color-corrected) fluxes, we list the predicted 24 and 70 μm fluxes integrated over the MIPS bandpasses in Table 3 and the significance of the deviation of the

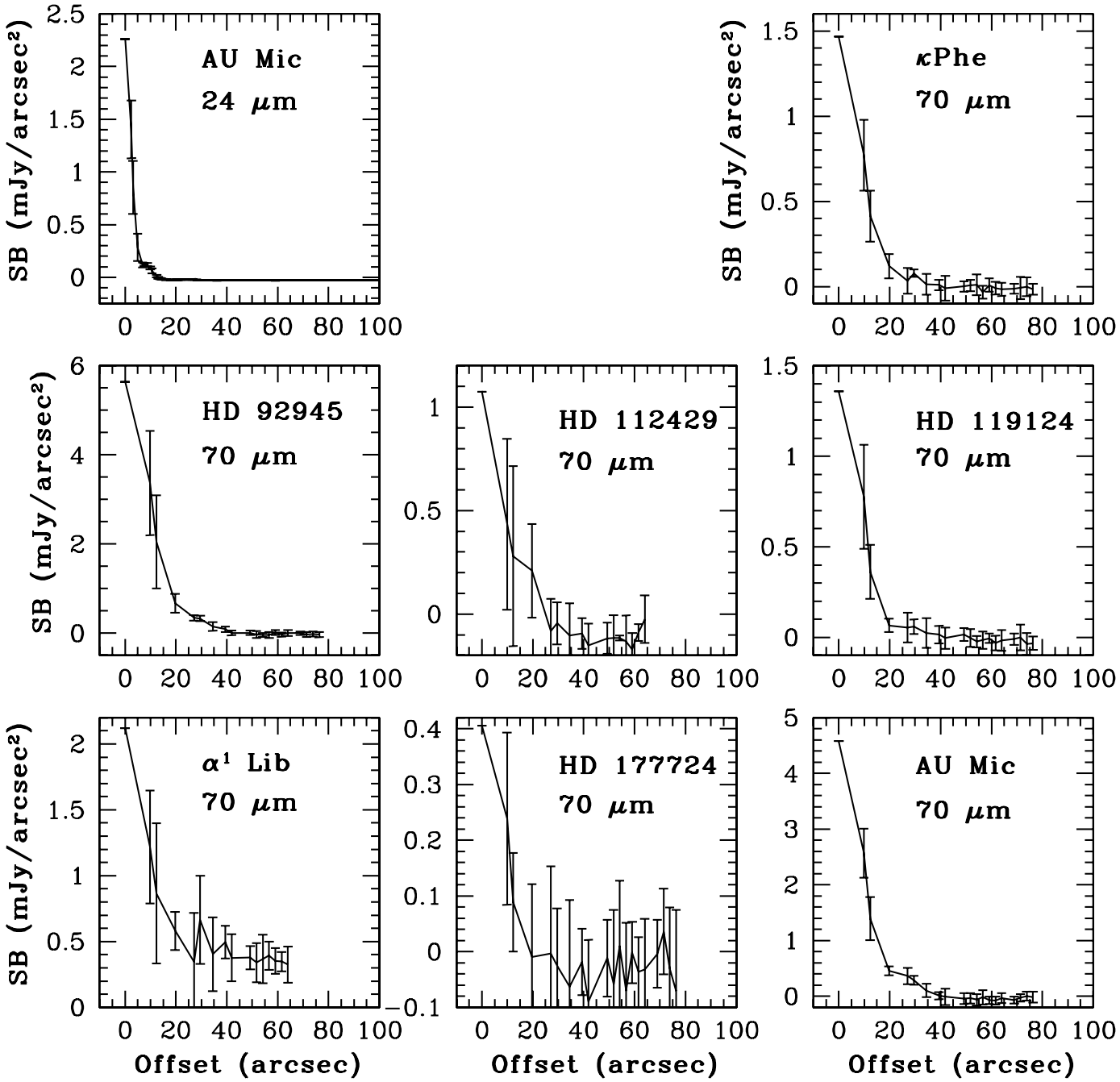

FIG. 3.—Azimuthally averaged radial profiles of HD 92945 at 24 μm (representative of all MIPS 24 μm detections in this study) and of the possible excess sources at 70 μm. Error bars represent the standard deviation in surface brightness at a given angular offset. All sources are point sources and have positions coincident with *Hipparcos* stellar positions, suggesting that the far-infrared emission is circumstellar and not interstellar.

measured flux, $\chi = [F_\nu\text{-}F_\nu(^*)]/\sigma_{F_\nu}$, at 24 and 70 μm. Histograms showing the distributions of $F_\nu/F_\nu(^*)$ and χ for both 24 and 70 μm are shown in Figure 4. We do not include stellar atmosphere models for M-type dwarfs because extrapolations of their photospheres from visual and near-infrared wavelengths has not yet been empirically verified. Instead, we compare the 2MASS K_s – [MIPS 24 μm] and the [MIPS 70 μm] – [MIPS 24 μm] colors (see Table 4) with *Spitzer* observations of dustless M-type dwarfs within 5 pc. For M0–M2 stars, Gautier et al. (2004) measure $\log[F_\nu(24\ \mu\text{m})/F_\nu(K_s)] = -1.8$. For M4 and M5 stars, Gautier et al. (2004) measure $\log[F_\nu(24\ \mu\text{m})/F_\nu(K_s)] = -1.7$ and $\log[F_\nu(70\ \mu\text{m})/F_\nu(24\ \mu\text{m})] = -0.95$. The measured $\log[F_\nu(24\ \mu\text{m})/F_\nu(K_s)]$values for the M-dwarfs in our sample are consistent to within 20% of the observations of Gautier et al. (2004). The measured 70 μm flux for AT Mic is 55% larger than what we predict based on the empirical M dwarf spectral energy distribution (SED); however, the AT Mic detection is only S/N = 5, and there is a high cirrus background in this region.

We detected all of the objects at 24 μm with a S/N > 100, and half of the objects (18 of 36) at 70 μm with a S/N $\geq$ 4. We expected to detect all of the stellar photospheres at 24 μm, and half of the stellar photospheres at 70 μm. MIPS 24 μm observations of Castor were not requested since they would have saturated the detector. Stars with 24 μm fluxes >20% above the photosphere and 70 μm fluxes >40% above the photosphere with a S/N > 10 are marked as excess objects in Table 3.

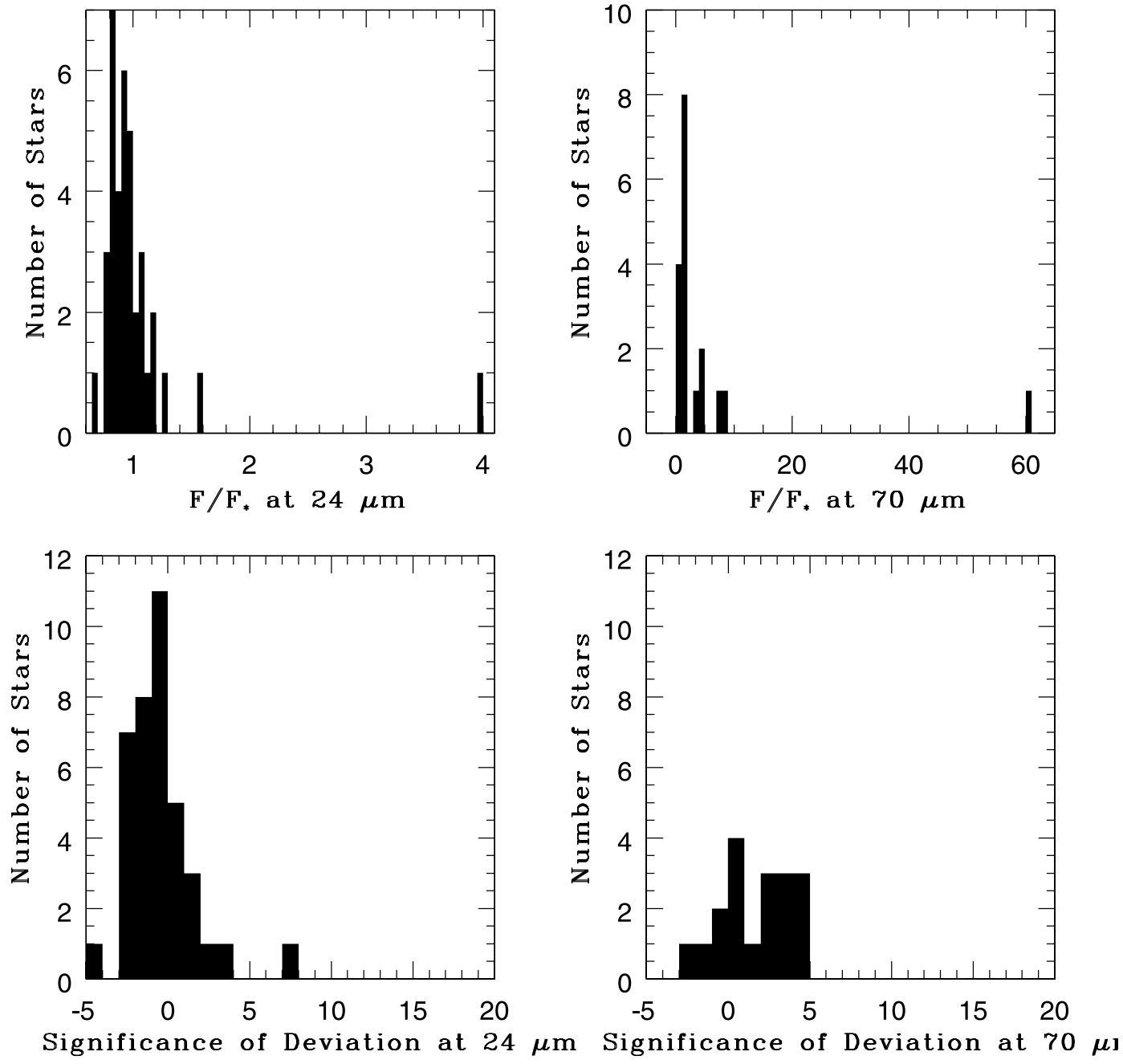

FIG. 4.—*Top:* Distribution of 24 and 70 μm fluxes relative to the expected photospheric values for all objects reported in this paper. *Bottom:* Statistical significance of deviations from the expected stellar fluxes at 24 and 70 μm.

TABLE 4
M DWARF MIPS COLORS

Name	Spectral Type	$\log[F_\nu(24\ \mu\text{m})/F_\nu(K_s)]$	$\log[F_\nu(70\ \mu\text{m})/F_\nu(24\ \mu\text{m})]$
Gl 182	M0	−1.89	<-0.29
RE 1816+541	dM1-2e	−1.89	<0.25
AT Mic	M4.5	−1.75	−0.76
AU Mic	M0	−1.83	0.12
HK Aqr	M0	−1.91	<0.042
	M1[a]	−1.83	−0.83
	M1.5[a]	−1.80	−0.96
	M3.5[a]	−1.75	−0.97

[a] From Gautier et al. (2004).

2.3. *CSO SHARC II Observations*

Our "long" wavelength observations were obtained using the SHARC II camera (Dowell et al. 2003) at the Nasmyth focus of the Caltech Submillimeter Observatory (CSO). Observations took place during exceptionally transparent (zenith $\tau_{225\ \mathrm{GHz}} = 0.032-0.037$) and stable conditions on 2005 April 22–23 UT. The Dish Surface Optimization System was active. The telescope was scanned in a Lissajous pattern with 60″ amplitude in azimuth and 40″ amplitude in elevation. The source image was reconstructed using the facility software CRUSH with the " deep" option appropriate for compact sources. The beam size after smoothing was 10″ FWHM. The telescope pointing was checked hourly and found to be repeatable to better than 3″ rms. We observed the two brightest 70 μm excess sources in our sample at 350 μm: HD 92945 and AU Mic. Calibration of HD 92945 was relative to TW Hya (6.6 Jy), Pallas (16.8 Jy), and Arp 220 (10.3 Jy). Calibration of AU Mic was relative to Neptune (93 Jy). The absolute calibration uncertainty is ~20%. Integration times were 2.5 and 1.8 hr on HD 92945 and AU Mic, respectively.

An unresolved 350 μm source is found to be coincident with HD 92945 within the ~2″ pointing accuracy of the telescope. For HD 92945, we measure $F_\nu(350\ \mu\mathrm{m}) = 60$ mJy, with a statistical uncertainty of 10 mJy and a calibration uncertainty of 12 mJy. AU Mic is marginally resolved at 350 μm with position angle ~135° and centroid within 3″ of the position of the star, consistent with scattered light imaging. For AU Mic, we measure $F_\nu(350\ \mu\mathrm{m}) = 72$ mJy, with a statistical uncertainty of 16 mJy and a calibration uncertainty of 14 mJy.

3. DISK PROPERTIES

Seven objects in our sample possess strong excesses at MIPS wavelengths. Four objects (κ Phe, HD 92945, HD 119124, and AU Mic), with estimated ages <50–200 Myr, possess strong 70 μm excesses, ≥100% larger than their predicted photospheres, and no 24 μm excesses, suggesting that the grains are cold. Both AU Mic and HD 92945 were bright enough to be detected by *Infrared Astronomical Satellite* (*IRAS*) at 60 μm and their excesses have been previously attributed to the presence of debris disks (Zuckerman & Song 2004; Song et al. 2002; Silverstone 2000). Scattered light observations of AU Mic have revealed the presence of an edge-on disk at distances between 50 and 210 AU (<21″) from the central star (Kalas et al. 2004). Gaussian fitting of the final image mosaics shows that the AU Mic 70 μm source size is not significantly larger than those of the other stars. Recently, follow-up *HST* Advanced Camera for Surveys scattered light observations have resolved an inclined disk with a radius 5″ around HD 92945 (J. Krist 2005, private communication). One object (HD 112429) possesses moderate 24 and 70 μm excesses with a blackbody color temperature, $T_{\mathrm{gr}} = 100$ K. Two objects (α^1 Lib and HD 177724) possess such strong 24 μm excess that their 12, 24, and 70 μm fluxes cannot be self-consistently modeled using a modified blackbody despite a 70 μm excess 2 times greater than the photosphere around α^1 Lib; therefore, the strong 24 μm excesses may be the result of emission in spectral features.

We use a modified blackbody to model the dust emission around κ Phe, HD 92945, HD 112429, HD 119124, and AU Mic. We have plotted *IRAS* fluxes, where available, on the SEDs in Figure 5 for comparison with our *Spitzer* fluxes. Models for the infrared and submillimeter emission of AU Mic suggest that dust grains around this star have a characteristic temperature $T_{\mathrm{gr}} = 40$ K, assuming an emissivity power-law index $\beta = 0.8$ (Liu et al. 2004). Our *Spitzer* MIPS and SHARC II photometry are consistent with this result. This model also appears to fit the 70 and 350 μm excess observed toward HD 92945. Since κ Phe and HD 119124 possess measured excesses at only 70 μm, we cannot place strong constraints on the dust emission around these objects. Instead, we fit a $T_{\mathrm{gr}} = 40$ K and $\beta = 0.8$ model to their SEDs. For HD 112429, we fit a blackbody to the excess fluxes, $\beta = 0$. We cannot confirm the presence of a 25 μm excess associated with Gl 182, inferred from reprocessed *IRAS* data (Liu et al. 2004). We observed Gl 182 at 160 μm and measured a 3 σ upper limit of <100 mJy. We did not observe any other targets at 160 μm.

The stars α^1 Lib and HD 177724 possess strong 24 μm excesses. The 12, 24, and 70 μm fluxes of these objects cannot be self-consistently modeled with a simple modified blackbody, with $\beta = 0.5-1.1$, even though α^1 Lib possesses a 70 μm excess >2 times the photospheric flux at this wavelength. The excess emission can be plausibly modeled if some of the emission is the result of spectral features. For α^1 Lac and HD 177724, we measure $F_\nu(24\ \mu\mathrm{m})/F_\nu(70\ \mu\mathrm{m}) = 11.0 \pm 2.5$ and $F_\nu(24\ \mu\mathrm{m})/F_\nu(70\ \mu\mathrm{m}) > 17.9$, respectively. If the grains were Draine & Lee astronomical silicates with $a = 1$ μm, then the dust would have temperatures, $T_{\mathrm{dust}} = 120-150$ K and $T_{\mathrm{dust}} > 170$ K, respectively, and distances, $D \sim 50$ AU and $D < 30$ AU, respectively. If the grains had an emissivity similar to that inferred for comet Hale-Bopp grains (Beichman et al. 2005b), then the dust would have temperatures, $T_{\mathrm{dust}} = 300-600$ K and $T_{\mathrm{dust}} > 870$ K, respectively, and distances, $D \sim 2.5-8$ AU and $D < 2$ AU, respectively. Recently, Beichman et al. (2005b) have observed the 1 Gyr old main-sequence K0 V star, HD 69830, with MIPS and the Infrared Spectrograph (IRS) on *Spitzer*. They find a strong 24 μm excess associated with the star. The infrared spectrum of this object reveals mid-infrared emission features nearly identical to those observed toward Hale-Bopp but with a higher grain temperature, $T_{\mathrm{gr}} = 400$ K instead of $T_{\mathrm{gr}} = 207$ K.

We list the estimated fractional infrared luminosities, L_{IR}/L_*, in Table 5. For objects with excesses detected at one wavelength (κ Phe, HD 119124, and HD 177724), we infer the fractional dust luminosities assuming $F_{\mathrm{IR}} \approx \nu F_{\mathrm{ex}}$, where F_{ex} is the excess flux at frequency ν. The fractional infrared luminosity may be higher if the grains produce more submillimeter emission than assumed. The fractional infrared luminosity for HD 92945, HD 112429, and AU Mic is found by integrating the thermal emission from the inferred blackbody. Our objects have $L_{\mathrm{IR}}/L_* = 7.3 \times 10^{-6}$ to 7.7×10^{-4} consistent with optically thin dust. The cold color temperatures of the grains around κ Phe, HD 92945, HD 112429, HD 119124, and AU Mic suggest that these systems may possess inner holes. Blackbodies in radiative equilibrium with a stellar source are located a distance

$$D = \frac{1}{2}\left(\frac{T_*}{T_{\mathrm{gr}}}\right)^2 R_* \qquad (1)$$

from the central star (Jura et al. 1998), where T_* and R_* are the effective temperature of the stellar photosphere and the stellar radius. Smaller grains radiate less efficiently and are therefore located at larger distances at the same temperature. We use stellar temperatures found in the literature. We estimate stellar luminosities, L_*, using *Hipparcos* V_T-band magnitudes and distances (in Table 1) and bolometric corrections from Flower (1996). We infer stellar radii from $L_* = 4\pi R_*^2 \sigma T_*^4$. From equation (1) and the stellar properties summarized in Table 1, we find the minimum grain distances listed in Table 5 all of which are ≤170 AU.

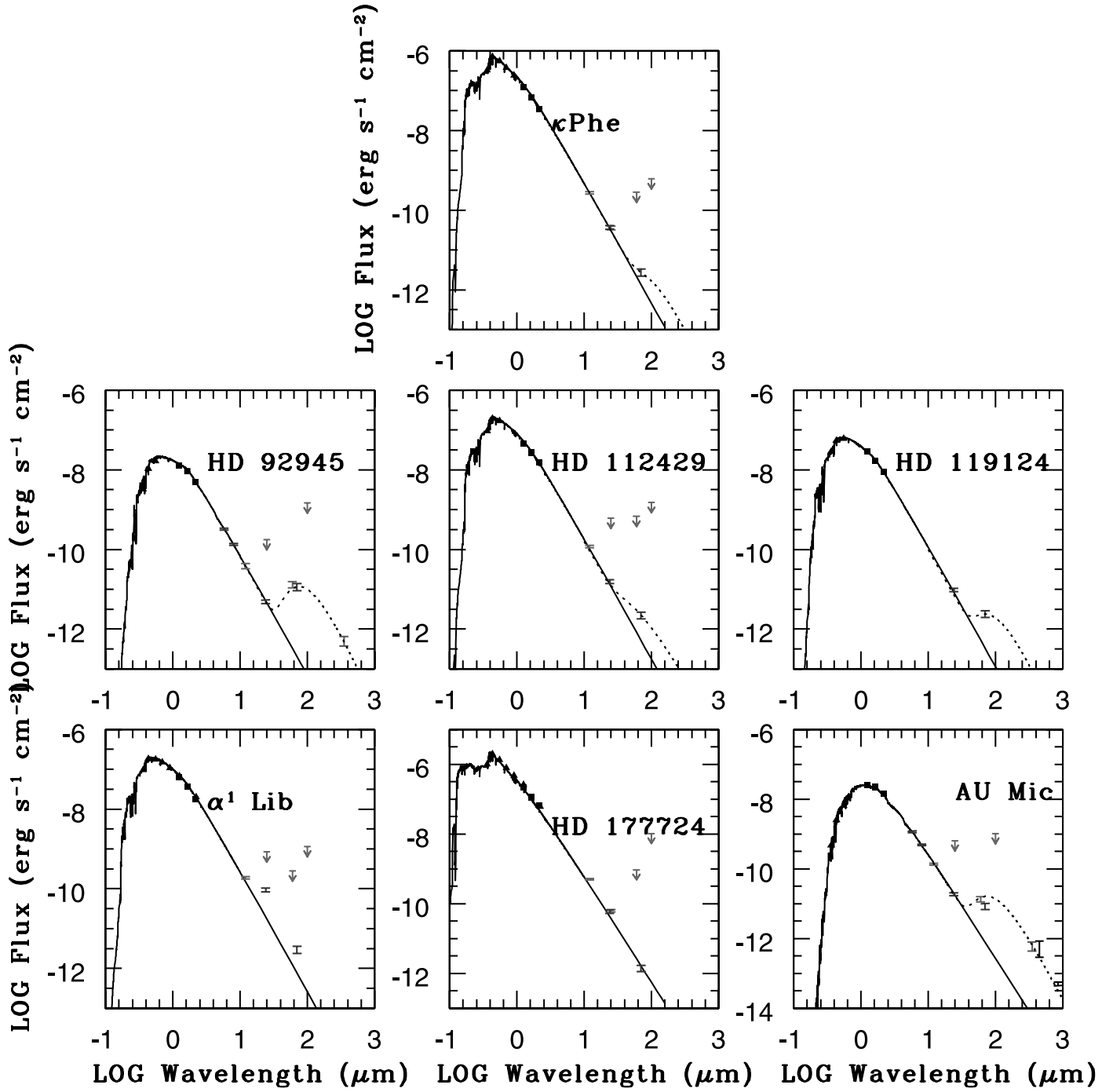

FIG. 5.—SEDs for stars with MIPS 24 and/or 70 μm excesses. GCPD mean *UBV* fluxes or Johnson et al. (1966) fluxes are plotted as triangles, and 2MASS *JHK* fluxes (Cutri et al. 2003) are plotted as squares. *IRAS* photometry, where available, is shown with light gray symbols. Our *Spitzer* 3.6–70 μm photometry and CSO SHARC II 350 μm photometry, as reported here, are shown with error bars. Overlaid are the best-fit 1993 Kurucz or Nextgen models for the stellar atmospheres. [*See the electronic edition of the Journal for a color version of this figure*.]

TABLE 5
OPTICALLY THIN DUST MODEL PARAMETERS

HD	T_* (K)	L_* ($L_\odot$)	R_* ($R_\odot$)	M_* ($M_\odot$)	T_{gr} (K)	L_{IR}/L_*	D_{min} (AU)	M_{dust} (M_{Moon})	$\dot{M}_{dust}$ (M_{Moon} yr^{-1})	M_{PB} (M_{Moon})
κ Phe	8000	11.8	1.8	1.8	40	2.0×10^{-6}	170	...	2×10^{-10}	0.04
HD 92945	5080	0.37	0.8	0.9	40	7.7×10^{-4}	30	2×10^{-3}	2×10^{-8}	1.5
HD 112429	7830	5.2	1.2	1.6	100	2.4×10^{-5}	20	2×10^{-4}	1×10^{-9}	0.05
HD 119124	6115	1.5	1.1	1.2	40	2.6×10^{-5}	60	6×10^{-4}	5×10^{-9}	0.9
α^1 Lib	6750	2.7	1.3	1.4	?	2.9×10^{-4}	...	...	3×10^{-8}	5.7
HD 177724	11912	61.9	1.9	2.9	?	7.3×10^{-6}	...	...	3×10^{-9}	0.25
AU Mic	3720	0.13	0.87	0.5	40	2.0×10^{-4}	20	1×10^{-4}	8×10^{-8}	5.9

4. MAIN-SEQUENCE A-TYPE STARS (e.g., HD 112429)

Three of our stars with IR excesses are A-type stars: κ Phe, HD 112429, and HD 177724. The high luminosity of main-sequence A-type stars plays a critical role in the removal of dust grains from debris disks. If the grains are small, then the grains are radiatively driven from the system. Large grains in low-density environments slowly spiral into their orbit center under Poynting-Robertson drag. Large grains in high-density environments collide, generating smaller fragments that may be radiatively driven from the system. We present a model to describe the circumstellar dust around any of the three A-type stars with infrared excess; however, we describe the model for HD 112429 as a specific example because the grain color temperature in this system has been constrained.

A lower limit to the size of dust grains orbiting a star can be found by balancing the force due to radiation pressure with the force due to gravity. For small grains with radius a, the force due to radiation pressure overcomes gravity for

$$a < 3L_* Q_{\rm pr}/(16\pi GM_* c\rho_s) \quad (2)$$

(Artymowicz 1988), where $Q_{\rm pr}$ is the radiation pressure coupling coefficient and ρ_s is the density of an individual grain. Since radiation from A-type stars is dominated by ultraviolet and visual light, we expect that $2\pi a/\lambda \gg 1$ and therefore the effective cross section of the grains can be approximated by their geometric cross section, so $Q_{\rm pr} \approx 1$. Based on $T_* = 7830$ K and $L_* = 5.2\ L_\odot$, the inferred stellar mass for HD 112429 is $1.6\ M_\odot$ (Siess et al. 2000). With $\rho_s = 2.5$ g cm^{-3}, the minimum radii for grains around HD 112429 is $a_{\rm min} = 0.8\ \mu$m.

We can estimate the average size of the grains assuming a size distribution for the dust grains. As expected from equilibrium between production and destruction of objects through collisions (Greenberg & Nolan 1989), we assume

$$n(a)da = n_o a^{-p} da, \quad (3)$$

with $p \simeq 3.5$ (Binzel et al. 2000). If we assume a minimum grain radius of 0.8 μm and weight by the number of particles, we find an average grain radius $\langle a\rangle = 1.3\ \mu$m. Since the size distribution of particles is not directly measured, the grains could be dominated by particles with a particular size, such as $a > 10\ \mu$m.

We can estimate the minimum mass of dust assuming that the particles have $\langle a\rangle \sim 1.3\ \mu$m; if the grains are larger or if the grains are at a larger distance, then our estimate is a lower bound. If we assume a thin shell of dust at distance, D, from the star and if the particles are spheres of radius, a, and if the cross section of the particles equals their geometric cross section, then the mass of dust is

$$M_d \geq \frac{16}{3}\pi \frac{L_{\rm IR}}{L_*}\rho_s D_{\rm min}^2 \langle a\rangle \quad (4)$$

(Jura et al. 1995), where $L_{\rm IR}$ is the luminosity of the dust. From equation (3) and the stellar properties summarized in Table 5, we infer dust masses, $M_{\rm dust} = 2\times 10^{-4} M_{\rm Moon}$.

One mechanism which may remove particles around main-sequence A-type stars is Poynting-Robertson drag. The Poynting-Robertson lifetime of grains in a circular orbit, a distance D from a star is

$$t_{\rm PR} = \left(\frac{4\pi\langle a\rangle\rho_s}{3}\right)\frac{c^2 D_{\rm min}^2}{L_*} \quad (5)$$

(Burns et al. 1979). For HD 112429, with the parameters given in Table 5, the Poynting-Robertson lifetime of grains is $t_{\rm PR} = 1.7\times 10^5$ yr. Since the Poynting-Robertson drag lifetime of the grains is significantly shorter than the estimated age of the system ($t_{\rm age} = 50$ Myr; Song et al. 2000, 2001), we hypothesize that the grains are replenished through collisions between larger bodies. Since the grains around α^1 Lib and HD 177724 are probably very warm, $T_{\rm dust} \sim 400$ K, the Poynting-Robertson drag lifetimes of the grains around these stars are probably also much shorter than the ages of these systems. Therefore, the material around these systems must also be replenished from a reservoir such as collisions between parent bodies or sublimation of comets. We cannot directly estimate the Poynting-Robertson drag lifetimes of these grains because their distances from their central stars are uncertain.

We can estimate the minimum mass contained in parent bodies around main-sequence A-type stars assuming a steady state and assuming that the dust removal rate can be inferred from the dust mass measured at mid- and far-infrared wavelengths and the Poynting-Robertson drag lifetime. If $M_{\rm PB}$ denotes the mass in parent bodies, then we may write

$$M_{\rm PB} \geq \frac{4L_{\rm IR} t_{\rm age}}{c^2} \quad (6)$$

(Chen & Jura 2001). If κ Phe, HD 112429, and HD 177724 have the properties listed in Table 5, then their parent-body masses, $M_{\rm PB} = 0.04 M_{\rm Moon} - 0.25 M_{\rm Moon}$.

5. MAIN-SEQUENCE SOLAR-LIKE AND M-TYPE STARS (e.g., HD 92945, HD 119124, AND AU MIC)

Unlike main-sequence A-type stars, radiation pressure, and Poynting-Robertson drag may not be the dominant forces clearing dust particles around solar-like main-sequence stars. Instead, the corpuscular stellar wind may remove small particles and stellar wind drag may effectively remove large dust particles around young solar-like stars (Chen et al. 2005) and around M-type stars (Plavchan et al. 2005). The increase in "drag" in the inward drift velocity, produced by stellar wind, over that produced by the Poynting-Robertson effect is given approximately by the factor $(1 + \dot{M}_{\rm wind} c^2/L_*)$, where $\dot{M}_{\rm wind}$ is the stellar wind mass loss rate (Jura 2004). We infer $\dot{M}_{\rm wind}$ from *ROSAT* fluxes using the observed dependence of stellar mass loss rate, $\dot{M}_{\rm wind}$, per stellar surface area, A, on X-ray flux per stellar area for nearby G-, K- and, M-type stars $\dot{M}_{\rm wind}/A \propto F_{\rm X}^{1.15\pm0.2}$ scaled to observations of 36 Oph ($F_{\rm X} = 3.6\times 10^5$ ergs cm^{-2} s^{-1}, $\dot{M}_{\rm wind}/A = 17\ \dot{M}_\odot/A_\odot$; Wood et al. 2002). Using the *ROSAT* fluxes listed in Table 1, we estimate $\dot{M}_{\rm wind} c^2/L_* = 56$, 64, and 2400 for HD 92945, HD 119124, and AU Mic, respectively, suggesting that stellar wind drag is more important than the Poynting-Robertson effect in these systems.

A lower limit to the size of dust grains orbiting a solar-like star can be found by balancing the radial force due to the corpuscular stellar wind with the force due to gravity. For small grains with radius, a, the force due to stellar wind drag overcomes gravity for

$$a < 3\dot{M}_{\rm wind} v_{\rm wind} Q_{\rm wind}/(16\pi GM_*\rho_s), \quad (7)$$

where $Q_{\rm wind}$ is the stellar wind coupling coefficient and $v_{\rm wind}$ is the wind velocity. In our solar system, $Q_{\rm wind} = 1$ and $v_{\rm wind} = 400$ km s^{-1}. If the stellar wind coupling coefficients and velocities are comparable around young, solar-like stars, we can estimate the minimum grain size in these systems. For the

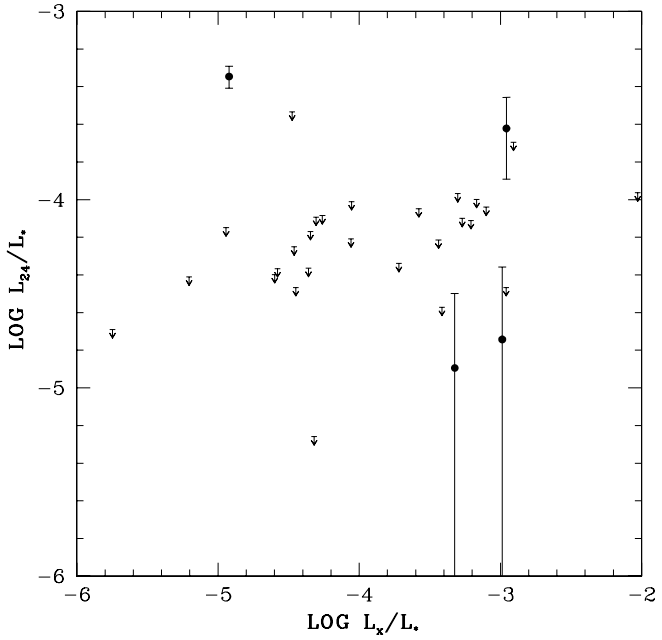

FIG. 6a

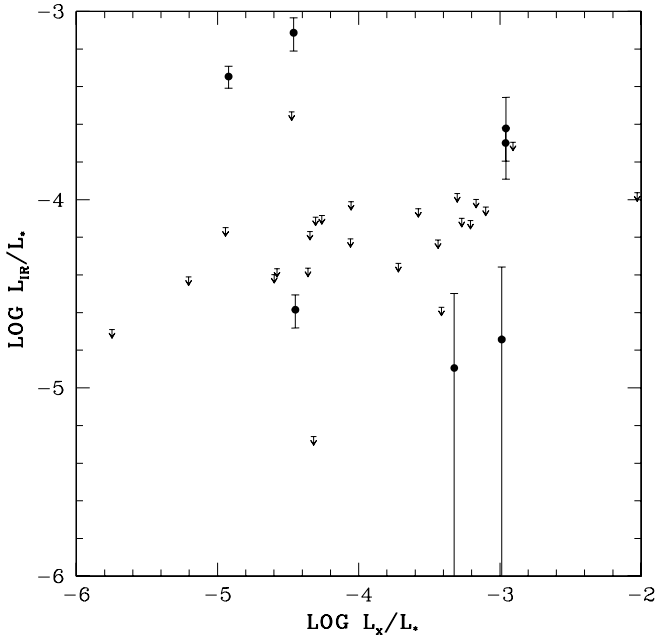

FIG. 6b

FIG. 6.—(*a*) Fractional infrared luminosity, as inferred from MIPS 24 μm photometry, plotted as a function of stellar X-ray luminosity. Objects plotted as filled circles have measured 24 μm fluxes that are larger than their predicted photospheric fluxes. For the remaining stars, 24 μm excess upper limits are estimated from the 3 σ uncertainty in the 24 μm flux. A-type stars have been excluded from this plot because the X-ray emission from this sources is probably produced by an undetected companion. (*b*) Same as (*a*), except that fractional infrared luminosity is calculated from both 24 and 70 μm fluxes if 70 μm excess is present.

stellar and grain parameters used above, the minimum radii for dust around HD 92945, HD 119124, and AU Mic are 0.01, 0.02, and 0.1 μm, respectively. For AU Mic, the minimum grain size under stellar wind drag is $\sim$1.3 times larger than that found by balancing radiation pressure with gravity. However, for HD 92945 and HD 119124, the minimum grain size under stellar wind drag is an order of magnitude smaller than the minimum grain size under radiation pressure, $a_{\rm min} = 0.1$ and 0.8 μm, respectively. If the grains in these systems have the same distribution as used above, then the mean grain size, $\langle a \rangle$, will be a factor of 5/3 larger than the minimum grain size.

We can estimate the minimum mass of dust assuming that the particles have $\langle a \rangle \sim 0.2$, 1.3, and 0.2 μm around HD 92945, HD 119124, and AU Mic; if the grains are larger or if the grains are at larger distances, then our estimates are a lower bound. If we use equation (4) and the values listed above, we estimate dust masses, $M_d = 2 \times 10^{-4} M_{\rm Moon}$ to $2 \times 10^{-3} M_{\rm Moon}$.

We can estimate the lifetime of circumstellar dust grains assuming that stellar wind drag is the dominant removal mechanism. If the grains are a distance, D, from the central star, then the stellar wind drag lifetime of grains in a circular orbit is

$$t_{\rm drag} = \frac{4\pi \langle a \rangle \rho_s D_{\rm min}^2}{3 \dot{M}_{\rm wind}} \quad (8)$$

(Chen et al. 2005). If HD 92945, HD 119124, and AU Mic, have $\dot{M}_{\rm wind}$ listed in Table 1 and $D_{\rm min}$ listed in Table 5, then the stellar wind drag lifetime of the grains is $t_{\rm drag} = 1.5 \times 10^4$ yr, 8.4×10^4 , and and 160 yr, respectively. AU Mic is a member of the β Pic moving group, age $\sim$12 Myr; HD 92945 is a member of the Local Association, age $\sim$20–150 Myr; HD 119124 is a member of the Castor moving group, age $\sim$200 Myr. Since the grain lifetimes against stellar wind drag are significantly shorter than the stellar ages, we hypothesize that the grains are replenished by collisions between larger bodies.

We can estimate the minimum mass contained in parent bodies around main-sequence solar-like stars assuming a steady state. If $M_{\rm PB}$ denotes the minimum parent-body mass, then we may write

$$M_{\rm PB} \geq \frac{L_{\rm IR}}{L_*} \dot{M}_{\rm wind} t_{\rm age} \quad (9)$$

(Chen et al. 2005). If HD 92945, HD 11924, and AU Mic have the properties listed above, then their parent-body masses, $M_{\rm PB} = 0.9 M_{\rm Moon} - 5.9 M_{\rm Moon}$. For comparison, the dust mass inferred to exist around AU Mic from SCUBA 850 μm observations is $\sim 0.9 M_{\rm Moon}$ (Liu et al. 2004), a factor of a few smaller than the $5.9 M_{\rm Moon}$ masses of parent bodies inferred to exist around this star.

6. DISCUSSION

Spitzer MIPS observations of young stars in Scorpius-Centarus suggest an anticorrelation between the fractional infrared luminosity, as inferred from 24 μm excess, and the fractional X-ray luminosity. Chen et al. (2005) suggest that this anticorrelation may be the result of stellar wind drag effectively removing dust grains from the circumstellar environment. We have plotted the fractional infrared luminosity, as inferred from MIPS 24 μm photometry, as a function of stellar X-ray luminosity (see Fig. 6*a*) to determine whether such an anticorrelation exists for this sample of stars. We exclude the A-type stars from this analysis because the X-ray emission seen along the line of sight toward these stars is likely associated with a later spectral-type companion. The majority of objects appear photospheric at 24 μm. Excluding α^1 Lib, only one other object may possess a weak 24 μm excess HD 358623. The statistical significance of 24 μm excesses associated with AB Dor/RST 137 and LO Peg are <1, suggesting that any excess associated with these stars is not statistically significant. Since none of the sources have substantial 24 μm excess, it

is difficult to comment with certainty about any correlation between 24 μm excess and X-ray luminosity. Some of our objects possess strong 70 μm excesses. Figure 6*b* includes both 24 and 70 μm data in the calculation of the IR luminosity—there is still no obvious correlation between X-ray flux and IR excess. However, because only a handful of stars are detected at MIPS wavelengths, our new data do not provide a strong test of the correlation proposed in Chen et al. (2005).

Dominik & Decin (2003) have suggested that the dust around main-sequence A-type stars may be in collisional equilibrium, which has been reached through a collisional cascade. While this paradigm may describe high fractional luminosity debris disks, $L_{\rm IR}/L_* = 10^{-4}$ to 10^{-3}, it may not describe the environments around low fractional luminosity debris disks $L_{\rm IR}/L_* = 10^{-5}$. For HD 112429, the collisional lifetime of the grains (2.3×10^5 yr) is slightly longer than the Poynting-Robertson lifetime of the grains (1.5×10^5 yr), suggesting that both processes may contribute to grain destruction. Dominik & Decin (2003) also argue that collisions may be less important for the grain evolution around lower mass stars because grains around lower mass stars experience fewer collisions. Indeed, micron-sized grains around AU Mic have a collisional lifetime of 3.9×10^4 yr, significantly longer than the inferred lifetime of grains under stellar wind drag (150 yr). However, like HD 112429, the collisional lifetimes of grains around HD 92945 and HD 119124 (1.8×10^4 yr and 1.3×10^5 yr) are commensurate with the grain lifetimes under stellar wind drag (1.5×10^4 and 8.4×10^4 yr), suggesting that both mechanisms may contribute to grain removal in these systems.

We estimate the parent-body masses around HD 92945, HD 112429, and HD 119124, assuming that radiation pressure is the dominant dust removal mechanism. Dust grains that are radiatively driven from the system reach a terminal velocity, $v_{\rm esc} = [2GM_*/D(\beta - 1)]^{1/2}$, where D is the distance at which the grains are produced (Su et al. 2005). The lifetime of the grains in the system can be inferred if we define grains at distances >1000 AU as lost to the system (Su et al. 2005). If we assume that the system is in steady state, and that the grain production rate is $M_{\rm dust}v_{\rm esc}/(1000\ {\rm AU})$, then the mass in parent bodies is $M_{\rm dust}v_{\rm esc}t_{\rm age}/(1000\ {\rm AU})$. For HD 92945, HD 1112429, and HD 119124, we estimate parent-body masses of $5.9M_{\rm Moon}$, $20M_{\rm Moon}$, and $390M_{\rm Moon}$. For HD 92945, the parent-body masses estimated assuming stellar wind drag and radiation pressure as the dominant mass removal mechanisms are similar to within a factor of a few. However, for HD 112429 and for HD 119124, the parent-body masses, inferred if radiation pressure is the dominant loss mechanism, are a 1000 times larger than predicted by other loss mechanisms. The inferred parent-body masses are somewhat large suggesting that the system may not be in steady state and that recent collisional cascades may have occurred.

The HD 92945 and AU Mic disks are observed to extend to radii of 5″ and 20″ (Kalas et al. 2004), respectively, in scatted light; however, the unresolved nature of the 70 μm emission suggests that the thermally emitting grains are located at a distance <6″, away from both stars. Since the simple blackbody grain model predicts grain distances 1.″3 and 2″, respectively, from the star, consistent with the observations, the 70 μm emission arising in both sources is likely due to thermal emission from large grains. Small grains, with $Q_{\rm abs} \propto 1/\lambda$, would be located a distance, $D = 0.5(T_*/T_{\rm gr})^{5/2} = 340$ AU (or 15″) from HD 92945 and 170 AU (or 17″) away from AU Mic. For AU Mic, the angular extent of the scattered light disk is consistent with small grains; however, for HD 92945, the angular extent of the scattered light grains is a factor of 3 smaller, suggesting that the grains in this system are larger. More sophisticated models are needed to elucidate the dust dynamics in these systems.

7. CONCLUSIONS

We have obtained *Spitzer Space Telescope* MIPS 24 and 70 μm photometry of 36 A- through M-type stars, with ages between 12 and 600 Myr, and IRAC 3.6, 4.5, 5.8, and 8.0 μm photometry for a subset of 11 stars.

1. Seven objects, with ages <50–200 Myr, possess 24 and/or 70 μm excesses, corresponding to a disk fraction ~18%, consistent with far-infrared observations of main-sequence stars. Larger studies of nearby, young stars are necessary to determine the disk dissipation timescale for solar-type stars.

2. We have detected 70 μm excess emission from cold dust around four stars (κ Phe, HD 92945, HD 119124, and AU Mic), and 24 and 70 μm excess emission from cool dust ($T_{\rm gr} = 100$ K) around HD 112429. In addition, we have detected strong 24 μm excess around α^1 Lib and HD 177724, despite the large 70 μm excess observed toward α^1 Lib, which may be the result of emission in spectral features. Follow-up IRS spectra are needed to determine whether the grain emissivity in these systems is similar to that of comet Hale-Bopp as observed toward HD 69830.

3. The grain lifetimes around the A-type star HD 112429 and around the solar-like stars HD 92945 and HD 119124 and around the M-dwarf AU Mic are much shorter than the stellar lifetimes, suggesting that the grains must be replenished by collisions between larger bodies. For all of these objects, except AU Mic, the collisional lifetimes of dust grains is similar to the Poynting-Robertson/stellar wind drag lifetimes of the grains, suggesting that both processes may be important in grain removal.

4. We do not detect infrared excess around any of our objects at 3.6–8.0 μm. We detect HD 92945 and AU Mic at submillimeter wavelengths and show that their 350 μm fluxes are consistent with our SED models. We resolve the emission from AU Mic at 350 μm with the same position angle as observed at other wavelengths.

We would like to thank M. Jura, K. Misselt, J. Stansberry, and our anonymous referee for their comments and suggestions. This work is based on observations made with the *Spitzer Space Telescope*, which is operated by the Jet Propulsion Laboratory, California Institute of Technology, under NASA contract 1407. Research at the Caltech Submillimeter Observatory is funded by NSF grant AST 02-29008.

REFERENCES

Allen, L. E., et al. 2004, ApJS, 154, 363
Artymowicz, P. 2988, ApJ, 335, 79
Barrado y Navascués, D. 1998, A&A, 339, 831
Beichman, C. A., et al. 2005a, ApJ, 622, 1160
———. 2005b, ApJ, 626, 1061
Binzel, R. P., Hanner, M. S., & Steel, D. I. 2000, in Allen's Astrophysical Quantities, ed. A. N. Cox (New York: AIP), 315
Burns, J. A., Lamy, P. L., & Soter, S. 1979, Icarus, 40, 1
Chen, C. H., & Jura, M. 2001, ApJ, 560, L171
Chen, C. H., Jura, M., Gordon, K. D., & Blaylock, M. 2005, ApJ, 623, 493
Cutri, R. M., et al. 2003, 2MASS All-Sky Catalog of Point Sources (Pasadena: IPAC/Caltech)
Dominik, C., & Decin, G. 2003, ApJ, 598, 626
Dowell, C. D., et al. 2003, Proc. SPIE, 4855, 73

Fazio, G. G., et al. 2004, ApJS, 154, 39
Fekel, F. C., Warner, P. B., & Kaye, A. B. 2003, AJ, 125, 2196
Flower, P. J. 1996, ApJ 469, 355
Gautier, T. N., et al. 2004, BAAS, 205, 5503
Gordon, K., et al. 2005, PASP, 117, 503
Gorlova, N., et al. 2004, ApJS, 154, 448
Gray, R. O., Corbally, C. J., Garrison, R. F., McFadden, M. T., & Robinson, P. E. 2003, AJ, 126, 2048
Gray, R. O., & Garrison, R. F. 1989, ApJS, 70, 623
Greenberg, R., & Nolan, M. C. 1989, in Asteroids II, ed. R. P. Binzel & T. Gehrels (Tucson: Univ. Arizona Press), 778
Heap, S. R., Lindler, D. J., Lanz, T. M., Cornett, R. H., Hubeny, I., Maran, S. P., & Woodgate, B. 2000, ApJ, 539, 435
Holland, W. S., et al. 2003, ApJ, 582, 1141
Jayawardhana, R., Fisher, S., Hartmann, L., Telesco, C., Pina, R., & Fazio, G. 1998, ApJ, 503, L79
Jeffries, R. D., James, D. J., & Bromage, G. E. 1994, MNRAS, 271, 476
Johnson, H. L., Mitchell, R. I., Iriarte, B., & Wisniewski, W. Z. 1966, Comm. Lunar Planet. Lab. 4, 99
Jura, M. 2004, ApJ, 603, 729
Jura, M., Ghez, A. M., White, Russell, J., McCarthy, D. W., Smith, R. C., & Martin, P. G. 1995, ApJ, 445, 451
Jura, M., Malkan, M., White, R., Telesco, C., Pina, R., & Fisher, R. S. 1998, ApJ, 505, 897
Kaisler, D., Zuckerman, B., Song, I., Macintosh, B. A., Weinberger, A. J., Becklin, E. E., Konopacky, Q. M., & Patience, J. 2004, A&A, 414, 175
Kalas, P., Liu, M., & Matthews, B. C. 2004, Science, 303, 1990
King, J. R., Villarreal, A. R., Soderblom, D. R., Gulliver, A. F., & Adelman, S. J. 2003, AJ, 125, 1980
Krist, J. 2002, Tiny Tim/SIRTF User's Guide (Pasadena: SSC)
Lagrange, A.-M., Backman, D. E., & Artymowicz, P. 2000, in Protostars and Planets IV, ed. V. Manning, A. P. Boss, & S. S. Russell (Tuscon: Univ. Arizona Press), 639
Lim, J. 1993, ApJ, 405, L33
Liu, M., Matthews, B. C., Williams, J. P., & Kalas, P. G. 2004, ApJ, 608, 526
Low, F. J., Smith, P. S., Werner, M. W., Chen, C. H., Krause, V., Jura, M., & Hines, D. 2005, ApJ, 631, 1170
Luhman, K., Stauffer, J. R., & Mamajek, E. E. 2005, ApJ, 628, L69
Marcy, G. W., Cochran, W. D., & Mayor, M. 2000, in Protostars and Planets IV, ed. V. Manning, A. P. Boss, & S. S. Russell (Tuscon: Univ. Arizona Press), 1285
Marsh, K. A., Velusamy, T., Dowell, C. D., Grogan, K., & Beichman, C. A. 2005, ApJ, 620, L47
Mermilliod, J.-C., Mermilliod, M., & Hauck, 1997, A&AS, 124, 349
Montes, D., López-Santiago, J., Gálvez, M. C., Fernández-Figueroa, M. J., De Castro, E., & Cornide, M. 2001, MNRAS, 328, 45
Plavchan, P., Jura, M., & Lipscy, S. J. 2005, ApJ, 631, 1161
Rieke, G., et al. 2004, ApJS, 154, 25
———. 2005, ApJ, 620, 1010
Royer, F., Grenier, S., Baylac, M.-O., Gómez, A. E., & Zorec, J. 2002, A&A, 393, 897
Schneider, G., et al. 1999, ApJ, 513, L127
Siess, L., Dufour, E., & Forestini, M. 2000, A&A, 358, 593
Silverstone, M. D. 2000, Ph.D. thesis, Univ. California (UCLA)
Song, I. 2000, Ph.D. thesis, Univ. Georgia
Song, I., Caillault, J.-P., Barrado y Navascués, D., & Stauffer, J. R. 2001, ApJ, 546, 352
Song, I., Caillault, J.-P., Barrado y Navascués, D., Stauffer, J. R., & Randich, S. 2000, ApJ 533, L41
Song, I., Weinberger, A. J., Becklin, E. E., Zuckerman, B., & Chen, C. H. 2002, AJ, 124, 514
Stapelfeldt, K. R., et al. 2004, ApJS, 154, 458
Su, K. Y. L., et al. 2005, ApJ, 628, 487
Telesco, C. M., et al. 2005, Nature, 433, 133
Thompson, G. I., Nandy, K., Jamar, C., Monfils, A., Houziaux, L., Carnochan, D. J., & Wilson, R. 1978, Catalog of Stellar Ultraviolet Fluxes (ESA SR-28; Noordwijk: ESA)
Wahhaj, Z., Koerner, D. W., Ressler, M. E., Werner, M. W., Backman, D. E., & Sargent, A. I. 2003, ApJ, 584, L27
Werner, M., et al. 2004, ApJS, 154, 1
Wood, B. E., Muller, H. R., Zanj, G. P., & Linsky, J. L. 2002, ApJ, 574, 412
Zuckerman, B., & Song, I. 2004 ApJ, 603, 738
Zuckerman, B., Song, I., & Bessell, M. S. 2004, ApJ, 612, L65
Zuckerman, B., Song, I., Bessell, M. S., & Webb, R. A. 2001, ApJ, 562, L87